Biochimica et Biophysica Acta, 983 (1989) 127–134
Elsevier

BBAMEM 74512

Low-conductance states of K^+ channels in adult mouse skeletal muscle

R. Weik, U. Lönnendonker and B. Neumcke

I. Physiologisches Institut der Universität des Saarlandes, Homburg (Saar) (F.R.G.)

(Received 11 November 1988)
(Revised manuscript received 9 February 1989)

Key words: Skeletal muscle; Patch clamp; Potassium ion channel; Low-conductance state; (Mouse)

Single-channel currents were recorded from Ca^{2+}-activated or ATP-sensitive K^+ channels in inside-out membrane patches excised from isolated mouse toe muscles. In addition to the closed and fully open configurations, both types of channels may exhibit several intermediate low-conductance states which are clustered near multiples of elementary conductance units. The units are 1/8 or 1/6 of the channel conductance for Ca^{2+}-activated channels and 1/4 or 1/3 for ATP-sensitive channels. Normally, low-conductance states are rare, but they occur more frequently directly after patch excision. An increased probability of low-conductance states of ATP-sensitive K^+ channels was also observed in the presence and during washout of the internal channel blocker adenine. The results suggest that Ca^{2+}-activated and ATP-sensitive K^+ channels are composed of several membrane pores with strong positive cooperativity among the elementary conductance units.

Introduction

Ionic channels in biological membranes are protein macromolecules forming an aqueous pore through the hydrophobic membrane interior. Normally, a channel exhibits only two conductance states (open, closed) and it opens and closes rapidly. Transitions between both states then produce step-like current traces between an upper and a lower level. Exceptions from such simple two-state conductance channels were described for the first time for channels opened by acetylcholine in embryonic muscle cells which may exhibit a sublevel between the main open configuration and the closed state [1]. Subsequently, subconductance states have been detected for a great variety of transmitter-regulated and voltage-gated cation- and anion-selective channels (for reviews, see Refs. 2 and 3).

This paper reports such low-conductance states for Ca^{2+}-activated and ATP-sensitive K^+ channels in adult mouse skeletal muscle. We describe conditions under which the states occur more frequently and give an analysis of their conductance values relative to the fully open state. It was found that the low-conductance states of both types of K^+ channels are not randomly distributed but are clustered near discrete steps of specified units. An attempt is made to relate this result to the recently derived structure of voltage-gated K^+ channels in *Drosophila* and in vertebrate brain.

Part of the results has been published as abstract [4].

Materials and Methods

Single skeletal muscle fibres were isolated from interosseal muscles of adult mice by treatment with collagenase (Sigma Type I, 3 mg/ml Ringer) at about 35°C for 2–3 h. The muscle fibres were transferred into tissue culture dishes and investigated with standard patch clamp recording techniques [5] as described previously for single frog skeletal muscle fibres [6].

All experiments were performed at room temperature (20–23°C) on excised membrane patches of the inside-out configuration using an L/M-EPC-5 amplifier (List, Darmstadt). The external solution (in the pipette) was composed of 155 mM KCl, 2 mM $CaCl_2$, 1 mM $MgCl_2$ (solution 1) or of 155 mM KCl, 3 mM $MgCl_2$, 0.5 mM EGTA (solution 2). The same results were obtained with both solutions. Normally, the bath solution on the sarcoplasmic side of the patches was mammalian Ringer (150 mM NaCl, 5 mM KCl, 2 mM $CaCl_2$, 1 mM

Abbreviations: ATP, adenosine 5′-triphosphate; EGTA, ethyleneglycol bis(β-aminoethyl ether)-*N*,*N*′-tetraacetic acid; Hepes, 4-(2-hydroxyethyl)-1-piperazineethanesulfonic acid.

Correspondence: B. Neumcke, I. Physiologisches Institut der Universität des Saarlandes, D-6650 Homburg (Saar), F.R.G.

$MgCl_2$). In some experiments (e.g., Figs. 1B, 7C) the bath solution was subsequently replaced with a K^+-rich internal solution (solution 1). All solutions were buffered with 5 or 10 mM Hepes and adjusted to pH 7.4 with KOH or NaOH. To block ATP-sensitive K^+ channels partly and reversibly, 5 mM adenine (Sigma, De senhofen) was added as free base to the internal solut on and washed out after 2–5 min.

Currents through K^+-selective ion channels were recorded on video tape. They were replayed and filtered by a four-pole low-pass Bessel filter set at one tenth of the sampling rate (10 to 30 kHz). A computer (DEC LSI 11/23) stored the data on winchester with the help of a DMA-Board (DT 2752, Data Translation). Selected segments of current traces were displayed and an initial value of the leakage current and the currents of all conductance states determined by cursor positioning. These current values were then used to detect and subtract the leakage current continuously and to classify the remaining channel currents into the various conductance levels by half-amplitude threshold analysis [7]. Two types of amplitude histograms ('raw' and 'excluded' histograms) of 100 bins were calculated simultaneously from the same (up to 134 s) periods of uninterrupted current recordings. In the 'excluded' type data points associated with transitions to and from different levels were omitted to confine the histogram to those points where the channel is open or closed. The rise time of the filter (time between 10 and 90% of a step transition, see Ref. 7) was used to define a time window before and after a transition, the points in which were excluded from the histogram. Thus currents immediately before and after a channel transition were discarded, whereas all currents during the various conductance states were considered without modification. Therefore, the peaks of the 'raw' and 'excluded' histograms were positioned at almost the same current values and both types of histograms had nearly a Gaussian shape. However, compared to 'raw' histograms, the peaks of the 'excluded' histograms were sharper and appeared more clearly on top of a reduced background level between peaks (see Fig. 2). Therefore, the analysis of the various conductance levels was performed with the 'excluded' type of amplitude histograms. As usual, currents in the amplitude histograms are plotted on the abscissa, the origin denotes the peak position of the closed-channel distribution and open-channel currents are assigned positive values. The histograms were fitted by the sum of Gaussian functions (see Figs. 2, 4 and 5). The peak positions and the standard deviations of the distributions were taken as the means and S.D. values of the respective current levels.

Potentials and currents are described by the physiological convention. Thus positive potentials mean positive on the sarcoplasmic side and positive currents correspond to an efflux of cations from the sarcoplasmic to the extracellular side.

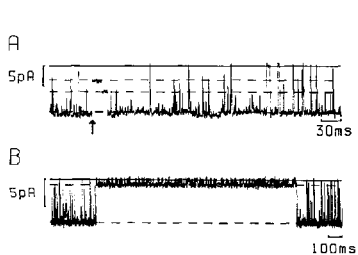

Fig. 1. Low-conductance states in Ca^{2+}-activated K^+ channels. The full lines denote the current level during channel closure and the lowest interrupted lines indicate currents during the fully open configuration. Low-conductance states are marked by intermediate interrupted lines. (A) Single-channel currents 10 min after excision at −50 mV, a transition to a low-conductance state is marked by an arrow. Internal solution: Ringer. Temperature 20 °C. Patch 121. (B) Currents 23 min after excision at −40 mV. The currents of the low-conductance-and of the fully-open-channel states as derived from the peaks in the amplitude histogram are −1.01 and −8.16 pA, respectively. Internal solution: solution 1. Temperature 20 °C. Patch 123.

Results

Excised membrane patches of adult mouse skeletal muscle contain several types of ionic channels. Of these we have identified two different K^+-selective channels [8] which are also present in other biological membranes. The first one requires Ca^{2+} ions in the internal solution for channel opening and is termed Ca^{2+}-activated K^+ channel; the second one is the so called ATP-sensitive K^+ channel because it is blocked selectively by ATP from the intracellular side (for a survey of different K^+ channels, see Ref. 9). As shown below, both types of K^+ channels in adult skeletal muscle can adopt various low-conductance states between the closed and the fully open conformations. Despite the large difference between the absolute conductances of the Ca^{2+}-activated and the ATP-sensitive K^+ channels there are remarkable similarities between the relative sizes of the low-conductance states in the two channels.

Ca^{2+}-activated K^+ channel

Figs. 1A, B illustrate short extracts of inward currents through Ca^{2+}-activated K^+ channels with Ringer (A) or the K^+-rich solution 1 (B) as internal solutions. In both cases rapid channel openings (plotted downward) and closures (plotted upward) occur between the current levels of the closed and fully open states. In addition, several intermediate conductance levels are adopted. For a systematic analysis of the various con-

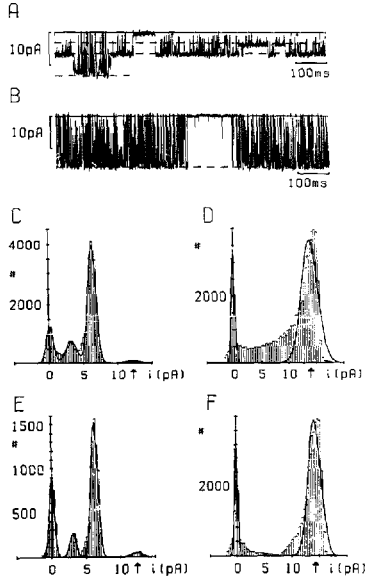

Fig. 2. Currents and amplitude histograms from a Ca^{2+}-activated K^+ channel shortly after patch excision (A, C, E) and about 1.5 min after excision (B, D, F). The full lines in (A, B) denote the current level during channel closure. The amplitude histograms were calculated from 12 s (C, E) and 21 s (D, F) periods of current recordings and show the number of sampled data points (#) as function of the current (i). (C, D) are 'raw' and (E, F) 'excluded' amplitude histograms calculated from the same periods of current recordings (see Methods). The currents of the fully open channel states as derived from the peaks in the 'excluded' histograms are −12.4 pA (E) and −14.3 pA (F). Membrane potential −60 mV. Internal solution: Ringer. Temperature 21°C. Patch 206.

ductance states amplitude histograms were calculated from long periods of continuous current recordings. Examples are shown in Fig. 2 together with representative segments of the periods. The results were obtained from the same Ca^{2+}-activated K^+ channel shortly after excision of the membrane patch from the muscle fibre (Figs. 2A, C, E) and about 1.5 min afterwards (Figs. 2B, D, F). The current records and the histograms illustrate the totally different channel behaviour at early and late times: During the first phase of channel activity the fully open state is only rarely adopted (Fig. 2A) and the corresponding peaks in the amplitude histograms C, E (marked by arrows) are very small. On the other hand, the same conductance level prevails at later times (Fig. 2B) and its peak in the amplitude histograms D, F even exceeds that of the closed channel state. The results illustrated in Fig. 2 were observed in a number of membrane patches but are not typical for all experiments. Instead, Ca^{2+}-activated K^+ channels normally exhibit the two-state behaviour of Fig. 2B directly after patch excision and show no obvious changes afterwards. However, if low-conductance states were observed at the beginning, they mostly and suddenly disappeared after some min. The transition between both gating modes was sometimes associated with a change of the current level of the fully open state (compare current values listed in the legend to Fig. 2). This change did not affect the analysis of the low-conductance states which were always determined from current records with intermediate levels and the fully open state.

The amplitude histograms shown in Figs. 2D, F are extreme cases with asymmetrical numbers of sampled data points on both sides of the amplitude peaks. The skewed distributions originate from fast flickery transitions between the closed and fully open channel configurations which do not reach the final current levels (see Fig. 2B). As a consequence, the peak position of the fitted Gaussian curve does not coincide with the most probable current amplitude. However, the difference is small for the 'raw' histogram of Fig. 2D, even smaller for the corresponding 'excluded' histogram of Fig. 2F and negligible in the majority of the analysed histograms.

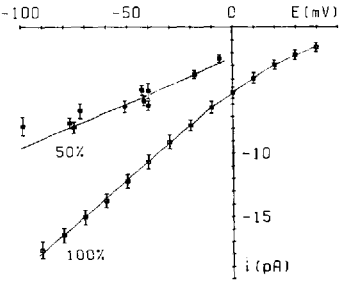

Fig. 3. Current (i)-voltage (E) curves of the 100% and 50% conductance levels of Ca^{2+}-activated K^+ channels. The symbols and bars represent mean values ± S.D. as obtained from the peak locations and widths of the respective distributions in amplitude histograms. The 100% values were obtained from measurements on patch 296, the 50% values from nine different patches. Internal solution: Ringer.

In the amplitude histograms of Figs. 2C, E the highest peaks are positioned at approximately half of the current corresponding to the fully open channel state. The 50% current level was also observed at other voltages and in Ca^{2+}-activated K^+ channels in other patches. Fig. 3 presents a summary of measurements on different membrane patches with Ringer as internal solution. The current-voltage curve of the fully open state (100%) is linear between -100 and -20 mV, has a slope of 145 pS in this voltage range and rectifies at more positive potentials owing to the presence of Na^+ ions in the internal solution. Measured half-amplitude currents are represented by filled squares and are close to the scaled 50% curve. This agreement suggests similar ionic selectivities of the 100% and 50% conductance states.

Ca^{2+}-activated K^+ channels may not only exhibit the 1/2 conductance level but also other intermediate states. Examples are shown in Figs. 1A, B and 2A. The small currents in the middle part of Fig. 1B are approximately 1/8 of the full sized currents on the left- and right-hand sides of the figure (compare current values listed in the legend to Fig. 1); multiples of these 1/8 conductance steps were found in this and other patches. Furthermore, conductances of 1/3 and 2/3 of the fully open state were observed. Fig. 4 illustrates that one single Ca^{2+}-activated K^+ channel may adopt the 2/3 and 1/2 conductance levels. The amplitude histograms were derived from currents at 0 mV recorded during two different time periods. Compared to the fully open state (arrows in Figs. 4A, B) the amplitude peaks of the low-conductance states are positioned near 2/3 (Fig. 4A) and 1/2 (Fig. 4B). A summary of all low-conductance states in Ca^{2+}-activated K^+ channels derived from experiments with Ringer as internal solution is given in the left-hand part of Fig. 6. In addition to the indicated conductance levels even smaller low-conductance states could be detected for Ca^{2+}-activated K^+ channels in some experiments. However, currents of these states could not be separated reliably from baseline currents, and this precluded a systematic analysis of the lowest conductance states.

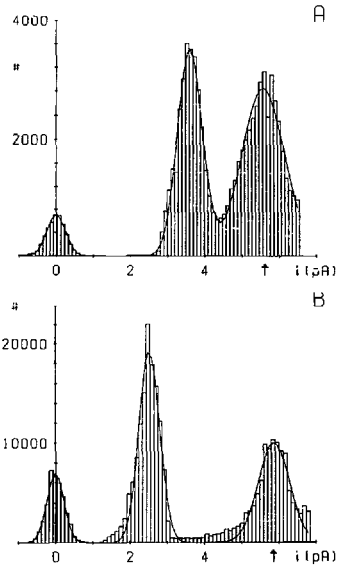

Fig. 4. Amplitude histograms of currents from Ca^{2+}-activated K^+ channels recorded 14 min (A) and 21 min (B) after patch excision. The current levels of the fully open state are marked by arrows, the peaks of the low-conductance states are located at 65% (A) and 43% (B) of the fully open state. The histograms were calculated from 48 s (A) and 65 s (B) periods of current recordings. Since the patch contained additional Ca^{2+}-activated K^+ channels without sublevels, the histograms were truncated on the right edges. Membrane potential: 0 mV. Internal solution: Ringer. Temperature 21° C. Patch 82.

ATP-sensitive K^+ channel

The different actions of intracellular Ca^{2+} and ATP on Ca^{2+}-activated and ATP-sensitive K^+ channels imply separate membrane structures for the two types of channels. Since the conductance of an ATP-sensitive channel is much lower than that of a Ca^{2+}-activated channel, the channels can be easily discriminated. Thus at -50 mV the current through an open ATP-sensitive channel is -3 pA (Fig. 5B) and through a Ca^{2+}-activated channel -12 pA under comparable conditions (Fig. 3). The records shown in Figs. 5A, B originate from ATP-sensitive K^+ channels shortly after the appearance of channel activity in the excised membrane patch (part A) and about 5.5 min later (part B). As in Ca^{2+}-activated K^+ channels (Fig. 2), there are frequent transitions to low-conductance states at the beginning, while only the closed and fully open states are adopted later. The different channel properties are reflected by the corresponding amplitude histograms in Figs. 5C, D which were calculated from long periods of currents recorded at early and late times, respectively. Since the channels are predominantly closed near -50 mV, the amplitude distribution of the closed state is by one order of magnitude higher than the peaks related to the open states. Therefore, the large numbers of sampled data points from the closed state have been omitted to

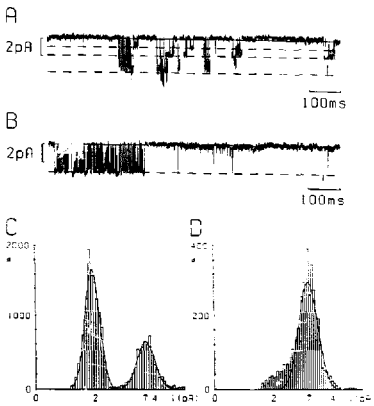

Fig. 5. Currents and amplitude histograms from an ATP-sensitive K^+ channel shortly after the appearance of channel activity at −55 mV (A, C) and about 5.5 min later at −50 mV (B, D). The full lines in (A, B) denote the current level during channel closure. The amplitude histograms were calculated from 134 s (C) and 40 s (D) periods of current recordings and do not contain data points from the closed-channel state. Internal solution: Ringer. Temperature 20 °C. Patch 114.

give a clearer presentation of the open-state amplitudes. The 1/4 conductance level visible in the records of Fig. 5A falls into the shoulder of the closed distribution and thus does not appear as a separate peak in the histogram of Fig. 5C.

As for Ca^{2+}-activated K^+ channels, the low-conductance states in ATP-sensitive K^+ channels were only observed in a minority of experiments and the probability of the intermediate states tended to decrease with time. In general, the analysis of the conductance levels in ATP-sensitive K^+ channels was more difficult than for Ca^{2+}-activated channels, because the channel currents were much smaller and a membrane patch often contained several ATP-sensitive channels. Despite these difficulties evidence for conductance levels in ATP-sensitive K^+ channels near 1/4, 1/2, 3/4 and 1/6, 1/3, 2/3 of the fully open state could be found in several experiments. The results obtained from measurements with Ringer as internal solution are summarized in the right-hand part of Fig. 6.

Low-conductance states in ATP-sensitive K^+ channels were observed more frequently in the presence of adenine in the internal solution and during washout of the base. Examples are shown in Fig. 7. The control currents in part A originate from at least three ATP-sensitive K^+ channels each switching between the closed and the fully open state. Addition of 5 mM adenine to internal Ringer produced a strong reduction of the open-probability of the channels (not shown). The

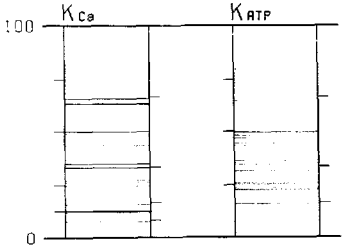

Fig. 6. Low-conductance states in Ca^{2+}-activated (K_{Ca}) and ATP-sensitive (K_{ATP}) K^+ channels. The conductance levels are plotted relative to the fully open (100%) state. The lines outside the columns mark the following levels: 12.5, 25, 50, 75% (K_{Ca}, left), 8.3, 16.7, 33.3, 66.7% (K_{Ca}, right), 25, 50, 75% (K_{ATP}, left), 16.7, 33.3, 66.7% (K_{ATP}, right). The lines within the columns indicate measured low-conductance states (26 determinations in Ca^{2+}-activated and 18 determinations in ATP-sensitive K^+ channels). All results were obtained from the location of peaks in amplitude histograms. Internal solution: Ringer.

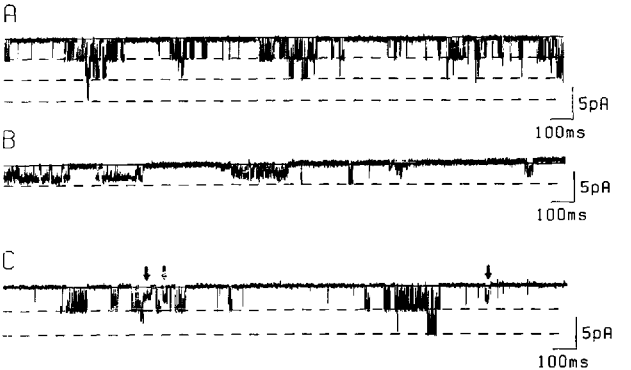

Fig. 7. Low-conductance states in ATP-sensitive K^+ channels in the presence and during washout of 5 mM internal adenine. (A) Control currents without adenine. The interrupted lines indicate current levels from one, two and three fully open channels. (B) Currents during washout of adenine, note frequent occurrence of flickery low-conductance states. (C) Currents in the presence of adenine, low-conductance states are marked by arrows. Membrane potential -40 mV (A, B) and -60 mV (C). Internal solutions: Ringer (A, B) and solution 1+5 mM adenine (C). Temperature 21°C (A, B and C). Patches 87 (A, B) and 135 (C).

blockage of ATP-sensitive K^+ channels by internal adenine was reversible, currents during the washout phase are shown in Fig. 7B. The records reveal numerous transitions to low-conductance states, while the fully open channel level (interrupted line in Fig. 7B) is only rarely reached. A more frequent occurrence of multiple conductance states in ATP-sensitive K^+ channels was also observed in the presence of adenine. This is illustrated by the currents in part C which are from a different patch and with 5 mM adenine in internal KCl solution.

Discussion

Two observations on low-conductance states in K^+ channels indicate that they are real channel properties and not artifacts produced by channels located under the rim of the patch pipette [10]: The intermediate states are always observed together with the fully open state (Figs. 1, 2, 5 and 7) and their conductance values are not random but are clustered around discrete steps of specified units (Fig. 6).

Low-conductance channel states may originate either from substates of a single population of channels or from separate channel populations. The frequently observed interconversions between the fully open and the low-conductance states and the occurrence of direct transitions crossing intermediate conductance levels (as marked by an arrow in Fig. 1A) suggest the existence of substates in Ca^{2+}-activated and ATP-sensitive K^+ channels.

Elementary conductance units

There are several reports on subconductance states of various types of K^+ channels in adult and cultured cells and in lipid bilayer membranes. In early investigations a single intermediate conductance level of about 40% the fully open state was described for Ca^{2+}-activated K^+ channels in rat myotubes [11] and a 1/3 conductance level for sarcoplasmatic reticulum K^+ channels in lipid bilayers [12]. Subsequently, multiples of elementary conductance units were found. Thus 1/3 and 2/3 levels occur in K^+ channels of smooth muscle [13] and 1/4, 1/2, 3/4 levels in inward rectifiers of heart ventricular cells [14] as well as in K^+ channels in the luminal membrane of renal tubules [15]. More examples are listed in a review [2]. Inwardly rectifying K^+ channels of cardiac myocytes may adopt the 1/3, 2/3 levels in some patches and 1/2, 3/4 levels in others [16]. According to our results (Fig. 4) a single Ca^{2+}-activated K^+ channel can switch between the 2/3 and 1/2 conductance levels during the course of an experiment. In addition, we have detected more low-conductance states in Ca^{2+}-activated K^+ channels with values near 1/8 and 1/6 of the fully open state (Figs. 1B, 6), and even smaller conductance states may exist for this type of

channel. Similarly, a division into approximately 16 conductance steps has been reported for K^+ channels in molluscan neurones [17].

Increased occurrence of subconductance states

Under normal conditions subconductance states in ionic channels are infrequent and their appearance is unpredictable. However, some manipulations may increase the occurrence of intermediate conductance states and facilitate their observation. Examples are the activation of multiple conductance states in synaptic receptors by excitatory amino acids in hippocampal [18] and cerebellar [19] neurons, the appearance of subconductance states in Na^+ channels after treatment with substances slowing the inactivation process [20,21] and the increased occurrence of low-conductance states in Ca^{2+} channels induced by cholesterol or lectins [22]. Furthermore, the probability of observing a subconductance state decreases with time after patch excision for large-conductance anion channels in B lymphocytes (M. Bosma, cited in Ref. 2) and for K^+ channels in skeletal muscle (this paper). Finally, numerous and frequently occurring low-conductance states are adopted in molluscan K^+ channels after application of an irreversible channel blocker [17] and in ATP-sensitive K^+ channels in the presence and during washout of a reversible blocker (Fig. 7).

Organization of K^+ channels

In general, low-conductance states in ionic channels can be explained with two different channel structures. The channel could be a single membrane pore of fluctuating diameter or the channel could be composed of several pores with a varying number of conducting units. In both cases, the lifetimes of the various channel conformations have to be much longer than the time for ion translocation through the channel and the conductance steps have to be larger than the thermal fluctuations to allow the observation of different conductance states [23]. An example of the first possibility of a single membrane pore is the ionic channel formed by the antibiotic alamethicin which appears to be composed of an oligomer of alamethicin molecules [24,25]. The observed transitions between neighbouring conductance levels have then been interpreted to arise from a variation in the number of molecules involved in the oligomer [24] or from conformational or position al changes within the preformed oligomer [25]. A similar structure of a K^+ channel with a single oligomeric pore seems to be less likely because it cannot account for the direct transitions between the closed and fully open states which are normally observed in K^+ channels. Furthermore, multiples of elementary conductance units are difficult to explain with a single pore. According to the absolute rate theory of membrane permeation [26] the channel current i is an exponential function of the height E of the main energy barrier in the channel. Hence, equal current increments Δi between low-conductance states do not correspond to uniform energy differences ΔE but would require a logarithmic division of E. Thus, while we cannot rule out definitely the single pore model, we favour the idea that a K^+ channel is organized as an aggregate of several pores. The individual pores in a channel may be separate barrels across the membrane phase as suggested for renal K^+ channels [15]. As an alternative, the pores could have separate mouths at one surface and merge into a single outlet at the other membrane side as inferred for porin channels [27]. Our experiments do not allow us to distinguish between the two possibilities. In any case, the individual pores within a K^+ channel should exhibit a strong positive cooperativity, because the frequently observed direct transitions between the closed and fully open channel states imply that all conductance units open and close simultaneously. Such a cooperativity among the pores in a channel explains our findings that K^+ channels normally exhibit a two-state behaviour and that the probabilities of the various conductance levels, therefore, deviate from a binomial distribution. Furthermore, strongly interacting pores in a channel can be hardly distinguished from a channel composed of a single pore. Thus the blockage of a K^+ channel by one toxin molecule or by one blocking ion can be interpreted with a single membrane pore as well as with an aggregate of interacting elementary subunits, since the presence of a blocking particle in one unit may be sensed by all other units. Direct evidence for interactions between conducting units within an ion channel has been obtained for L-type Ca^{2+} channels incorporated into lipid bilayer membranes which originate from the aggregation of low-conductance monochannels to an oligomer with strict functional coupling among the associated monomers [28].

The proposed multi-barrel model for Ca^{2+}-activated and ATP-sensitive K^+ channels does not only account for the observed multiples of elementary conductance units, but it also gives a natural explanation for the increased occurrence of subconductance states induced by physical or chemical interventions. Thus, asynchronous opening and closing of the individual pores in a channel could arise from distortions in the surrounding lipid environment caused by the excision of the membrane patch or by treatment with cholesterol or lectins. Furthermore, substances facilitating channel opening, modifying channel gating or blocking channels could reach and affect each pore separately and thereby increase the appearance of low-conductance states.

The number of pores in a Ca^{2+}-activated or in an ATP-sensitive K^+ channel may be rather large as estimated from the observed low-conductance states. For example, a 1/8 conductance step in a Ca^{2+}-activated channel (Fig. 1B) could be interpreted by the presence

of eight identical pores. However, different pores in a channel may have different elementary conductances, and this precludes an estimate of the number of pores in a Ca^{2+}-activated K^+ channel. The same uncertainty applies to ATP-sensitive K^+ channels. The aggregation of equal or different subunits in a K^+ channel is hypothetical, but it can be related to the recently derived structure of voltage-gated K^+ channels in *Drosophila* [29] and in mouse [30] and rat [31] brain. According to these results, a K^+ channel may be a homo- or hetero-oligomer formed by the aggregation of many separate subunits [32]. This channel structure provides a maximum flexibility for a large number of pores within or between the channel subunits, and this could account for the multiplicity of the low-conductance states in Ca^{2+}-activated and ATP-sensitive K^+ channels.

Acknowledgements

We thank Professor H. Meves and Dr. T. Plant for reading the manuscript and for many helpful comments. We are grateful to Dr. P. Krippeit-Drews and Ms. B. Jung for valuable advice in the preparation of single muscle fibres, to Dr. D. Hof for assistance in hard- and software problems and to Mrs. B. Schwarz for secretarial help. This research was supported by the Deutsche Forschungsgemeinschaft (SFB 246 and Ne 287/3-2).

References

1 Hamill, O.P. and Sakmann, B. (1981) Nature 294, 462–464.
2 Fox, J.A. (1987) J. Membr. Biol. 97, 1–8.
3 Meves, H. and Nagy, K. (1989) Biochim. Biophys. Acta 988, 99–105.
4 Neumcke, B. and Weik, R. (1988) Pflügers Arch. 412 (Suppl. No. 1), R14.
5 Hamill, O.P., Marty, A., Neher, E., Sakmann, B. and Sigworth, F.J. (1981) Pflügers Arch. 391, 85–100.
6 Woll, K.H., Leibowitz, M.D., Neumcke, B. and Hille, B. (1987) Pflügers Arch. 410, 632–640.
7 Colquhoun, D. and Sigworth, F.J. (1983) in Single-Channel Recording, (Sakmann, B. and Neher, E., eds.), Plenum Press, New York.
8 Neumcke, B., Lönnendonker, U. and Woll, K.H. (1988) Ber. Bunsenges. Phys. Chem. 92, 1028–1031.
9 Rudy, B. (1988) Neuroscience 25, 729–749.
10 Neher, E., Sakmann, B. and Steinbach, J.H. (1978) Pflügers Arch. 375, 219–228.
11 Barrett, J.N., Magleby, K.L. and Pallotta, B.S. (1982) J. Physiol. (Lond.) 331, 211–230.
12 Labarca, P.P. and Miller, C. (1981) J. Membr. Biol. 61, 31–38.
13 Benham, C.D. and Bolton, T.B. (1983) J. Physiol. (Lond.) 340, 469–486.
14 Sakmann, B. and Trube, G. (1984) J. Physiol. (Lond.) 347, 641–657.
15 Hunter, M. and Giebisch, G. (1987) Nature 327, 522–524.
16 Matsuda, H. (1988) J. Physiol. (Lond.) 397, 237–258.
17 Kazachenko, V.N. and Geletyuk, V.I. (1984) Biochim. Biophys. Acta 773, 132–142.
18 Jahr, C.E. and Stevens, C.F. (1987) Nature 325, 522–525.
19 Cull-Candy, S.G. and Usowicz, M.M. (1987) Nature 325, 525–528.
20 Chinn, K. and Narahashi, T. (1986) J. Physiol. (Lond.) 380, 191–207.
21 Nagy, K. (1987) Eur. Biophys. J. 15, 129–132.
22 Ma, J. and Coronado, R. (1988) Biophys. J. 53, 387–395.
23 Läuger, P. (1985) Biophys. J. 47, 581–591.
24 Boheim, G. (1974) J. Membr. Biol. 19, 277–303.
25 Gordon, L.G.M. and Haydon, D.A. (1976) Biochim. Biophys. Acta 436, 541–556.
26 Parlin, B. and Eyring, H. (1954) in Ion Transport across Membranes, (Clarke, H.T., ed.), Academic Press, New York.
27 Engel, A., Massalski, A., Schindler, H., Dorset, D.L. and Rosenbusch, J.P. (1985) Nature 317, 643–645.
28 Hymel, L., Striessnig, J., Glossmann, H. and Schindler, H. (1988) Proc. Natl. Acad. Sci. USA 85, 4290–4294.
29 Schwarz, T.L., Tempel, B.L., Papazian, D.M., Jan, Y.N. and Jan, L.Y. (1988) Nature 331, 137–142.
30 Tempel, B.L., Jan, Y.N. and Jan, L.Y. (1988) Nature 332, 837–839.
31 Baumann, A., Grupe, A., Ackermann, A. and Pongs, O. (1988) EMBO J. 7, 2457–2463.
32 Agnew, W.S. (1988) Nature 331, 114–115.